

Origin of the metallicity distribution of the NGC 5128 stellar halo

K. Bekki,¹ William E. Harris^{2,4}, and Gretchen L. H. Harris^{3,4}

¹*School of Physics, University of New South Wales, Sydney 2052, NSW, Australia*

²*Department of Physics & Astronomy, McMaster University, Hamilton ON L8S 4M1, Canada*

³*Department of Physics, University of Waterloo, Waterloo ON N2L 3G1, Canada*

⁴*Visiting Fellow, Research School of Astronomy & Astrophysics, Australian National University, Weston, ACT 2611, Australia*

Accepted Received in original form 2001

ABSTRACT

Recent *Hubble Space Telescope* photometry in the nearby elliptical galaxy NGC 5128 shows that its halo field star population is dominated by moderately metal-rich stars, with a peak at $[m/H] \simeq -0.4$ and with a very small fraction of metal-poor ($[m/H] < -1.0$) stars. In order to investigate the physical processes which may have produced this metallicity distribution function (MDF), we consider a model in which NGC 5128 is formed by merging of two major spiral galaxies. We find that the halo of an elliptical formed this way is predominantly populated by moderately metal-rich stars with $[m/H] \sim -0.4$ which were initially within the outer parts of the two merging discs and were tidally stripped during the merger. To match the NGC 5128 data, we find that the progenitor spiral discs must have rather steep metallicity gradients similar to the one defined by the Milky Way open clusters, as well as sparse metal-poor haloes (5% or less of the disc mass). Very few stars from the central bulges of the spiral galaxies end up in the halo, so the results are not sensitive to the relative sizes (bulge-to-disc ratios) or metallicities of the initial bulges. Finally, we discuss the effects on the globular cluster system (GCS). The emergent elliptical will end up with metal-poor halo clusters from the original spiral haloes, but with moderately metal-rich halo stars from the progenitor discs, thus creating a mean offset between the MDFs of the halo stars and the GCS. Remaining questions yet to be answered concern the total size of the GCS population (the “specific frequency problem”) and the observed existence of metal-rich globular clusters in large numbers in the outer haloes of giant ellipticals. We also discuss possible differences in the MDFs of stellar haloes of galaxies of different Hubble type.

Key words: galaxies:abundances — galaxies:elliptical and lenticular, cD — galaxies:evolution — galaxies:individual (NGC 5128) — galaxies:stellar content — globular clusters:general

1 INTRODUCTION

Physical properties of metal-deficient stellar haloes in galaxies are considered to provide vital clues to the understanding of early dynamical and chemical evolution of galaxies. In particular, the detailed investigation of structural, kinematic, and chemical properties of such a “fossil record” component (i.e., stellar halo) of the Galaxy has revealed a possible scenario as to how the Galaxy has developed its dynamical structures such as bulge, thin and thick discs (e.g., Freeman 1987; Majewski 1993; van den Bergh 1996). Because of the observational difficulties in revealing three dimensional structure and kinematics of halo stars (with respect to their

host galaxy) in each of the Local Group galaxies other than the Milky Way, the metallicity distribution function (hereafter MDF) of halo stars in these galaxies has served to give some constraints on the past star formation and chemical evolution histories of these systems (Mould & Kristian 1986; Durrell, Harris, & Pritchet 1994, 2001; Pritchet & van den Bergh 1998; Christian & Heasley 1986; Reitzel, Guhathakurta, & Gould 1998; Grillmair et al. 1996; Han et al. 1997; Martinez-Delgado & Aparicio 1998). The stellar halo of M31 appears to be dominated by a moderately high-metallicity population with $[m/H] \sim -0.5$ (cf. the references cited above), a strikingly different enrichment level than in the Milky Way stellar halo, and a strong indicator of

a different formation history (e.g. Durrell, Harris, & Pritchett 2001).

Although there have been many MDF studies of halo stars in Local Group members, galaxies beyond the Local Group have only recently been investigated through *HST*/WFPC2 photometry and for only a small number of cases: the giant E/S0 NGC 5128 (Soria et al. 1996; Harris, Harris, & Poole 1999 hereafter referred to as HHP; Harris & Harris 2000, HH00; Harris & Harris 2002, HH02; Marleau et al. 2000), the edge-on S0 NGC 3115 (Elson 1997; Kundu & Whitmore 1998), and two dwarf ellipticals in the M81 group (Caldwell et al. 1998). Furthermore, Rejkuba et al. (2002) have demonstrated the existence of a significant intermediate-age AGB population in parts of the NGC 5128 halo, based on deep *U*, *V*, and *K_s* color-magnitude and color-color diagrams of halo stars resolved by VLT.

A remarkable result emerging from the *HST*/WFPC2 photometry of the old-halo red giant stars in NGC 5128 is the dominance of moderately metal-rich stars in the range $-1 < [\text{m}/\text{H}] < 0.0$ (HHP, HH00, and HH02). HH00 and HH02 suggested that the relatively high mean abundance and small fraction ($\sim 10\%$) of metal-poor stars with $[\text{m}/\text{H}] < -1$ can give strong constraints on the total mass of dwarf galaxies that could be accreted by NGC 5128 and then disrupted to form its faint stellar halo.

To date, however, there are only a few attempts at physical interpretation of this material. HH00 discussed a one-zone model of chemical evolution of this galaxy and suggested that it experienced two fairly distinct stages of halo formation: an early “accreting box” stage when the galaxy is assembling through infall of star-forming gas clumps, and then a major stage of “closed-box” evolution when the star formation proceeds in the galaxy with little gas infall. HH02 extended this basic picture further to a more generalized accreting-box formation model, in which the infall rate of unenriched gas is envisaged to start at a high rate and then dies away exponentially, while star formation continues throughout until the gas supply is exhausted. With appropriate choices of gas infall rate and the effective chemical yield, excellent overall matches to the observed MDFs can be obtained. Recently, Beasley et al. (2002a, b) have further discussed the origin of the stellar halo MDF within the context of a semi-analytic model of galaxy formation (GALFORM), based on the Cold Dark Matter (CDM) picture. In this model, star formation can take place in two modes, a “quiescent” mode within the relatively unenriched pregalactic clouds, and a “starburst” mode whenever two roughly equal clouds suddenly merge. They demonstrated that the global metallicity distribution within model galaxies comparable to NGC 5128 in size is broadly consistent with the observed MDF, although the model is unable to provide any information on the spatial distribution or radial change in the MDF.

These previous studies are based on one-zone models of chemical evolution and thus cannot spatially resolve the various distinct stellar components (i.e., halo, bulge, and disc) in a galaxy. Accordingly, comparisons of these models with the MDFs observed at different places in NGC 5128 have limited value. Numerical simulations which enable us to resolve spatially the halo, bulge, and disc components and thereby to investigate the MDF for each of these com-

ponents should be very helpful for better understanding the formation of galactic stellar haloes.

The purpose of this paper is to investigate the origin of the MDF of the stellar halo of NGC 5128 based on numerical simulations of elliptical galaxy formation. We here adopt the basic “merger” approach (Toomre 1977) in which elliptical galaxies are proposed to be formed by major merging of two spiral galaxies. Within the context of this assumption, we investigate the final MDF of the outer halo component of the merger remnant (i.e., the giant E galaxy) as well as its dependence on the input parameters of the progenitor discs (e.g., the MDFs of discs, bulge-to-disc-ratio, and halo mass fraction of the disc). Comparing the simulated MDFs with the observed ones for NGC 5128, we discuss the following points: (1) how the dynamics of galaxy merging is important for the formation of the gE stellar halo, (2) how the initial MDF of a disc (or bulge) in a merger controls the final MDF of the stellar halo, (3) whether the bulge-to-disc ratio of a merger progenitor spiral is important for the determination of the stellar halo’s MDF, (4) what initial conditions of galaxy mergers in the present simulations can best give the MDF similar to the observed one, (5) the relevance of the MDF for the globular cluster system, which is different from the field-halo stars, and (6) whether, on the grounds of the merger picture, we should always expect the MDFs of stellar haloes in elliptical galaxies (E) to be systematically different (more metal-rich) from those in late-type spirals (Sp).

The plan of the paper is as follows: In the next section, we describe our numerical models for stellar halo formation in galaxy mergers. In §3, we present the numerical results mainly on the final MDFs of merger remnants (i.e., elliptical galaxies) for variously different merger models. In §4, we predict a possible relationship between MDFs of stellar haloes and physical properties of their host elliptical galaxies. In this section, we also discuss the origin of M31’s metal-rich stellar halo. We summarize our conclusions in §5.

2 THE MODEL

2.1 Merger model parameters

In the model calculations, we numerically investigate dynamical evolution of major galaxy mergers between spiral galaxies whose primary components are dark matter haloes, stellar discs, stellar haloes, and globular clusters (GCs). In the present study, we do not include gaseous components (thus no star formation) in the simulations so that all of the halo stars in the merger remnant come from the pre-existing stellar components of the progenitor spirals. The density profiles of dark matter and disc components in a spiral follow the Fall-Efstathiou (1980) model. The total mass and the size of a disc are assumed to be M_d and R_d , respectively. All masses and lengths are measured in units of M_d and R_d unless otherwise specified. Velocity and time are measured in units of $v = (GM_d/R_d)^{1/2}$ and $t_{\text{dyn}} = (R_d^3/GM_d)^{1/2}$, respectively, and the gravitational constant G , is assumed to be 1.0. If we adopt $M_d = 6.0 \times 10^{10} M_\odot$ and $R_d = 17.5$ kpc as fiducial values, then $v = 1.21 \times 10^2$ km/s and $t_{\text{dyn}} = 1.41 \times 10^8$ yr.

In the disc model, the rotation curve becomes nearly

flat at $R = 0.35$ (where R is distance from the centre of the disc) with the maximum rotational velocity $v_m = 1.8$ in our units (220 km s^{-1}). The corresponding total mass of the dark matter halo (within $1.5R_d$) is 4.0 in our units. The velocity dispersion of the dark halo component at a given point is set to be isotropic and given according to the virial theorem. The radial (R) and vertical (Z) density profiles of the disc are assumed to be proportional to $\exp(-R/R_0)$ with scale length $R_0 = 0.2$ and to $\text{sech}^2(Z/Z_0)$ with scale length $Z_0 = 0.04$ in our units, respectively. In addition to the rotational velocity caused by the gravitational field of disc, bulge, and dark halo components, the initial radial and azimuthal velocity dispersions are assigned to the disc component according to the epicyclic theory with Toomre's parameter $Q = 1.5$. The vertical velocity dispersion at given radius is set to be 0.5 times as large as the radial velocity dispersion at that point, as is consistent with the observed trend of the Milky Way (e.g., Wielen 1977).

The density profile of the central bulge with a mass of M_b and effective radius of R_e (in our units) is represented by the de Vaucouleurs $R^{1/4}$ law. We mainly investigate two different bulge models: (a) a model with $M_b = 0.2$ (in our units, corresponding to $1.2 \times 10^{10} M_\odot$) and $R_e = 0.04$ (in our units corresponding to 0.7 kpc) and (b) a model with $M_b = 0.6$ ($3.6 \times 10^{10} M_\odot$) and 0.11 (2 kpc). These two cases are intended to correspond roughly to the Milky Way and to M31, respectively. Each spiral is assumed to have an extended stellar halo with a density distribution of $\rho(r) \sim r^{-3.5}$, where r is the distance from the center of the spiral. The mass fraction of the stellar halo is represented by f_h and considered to be a free parameter in the present study.

We also include a population of collisionless particles to represent a part of the globular cluster system in each galaxy. The Milky Way and M31 are observed to have 160 ± 20 and 400 ± 55 globular clusters, respectively (van den Bergh 1999). We therefore assume each spiral to have 200 old, metal-poor globular clusters with a number density distribution like that of the Milky Way system (i.e., $\rho(r) \sim r^{-3.5}$).

In total, the numbers of particles used for modeling the merger are 20000 for the dark matter haloes, 20000 for the discs, 12000 (4000) for bulges (The Galactic bulge), 4000 for the stellar haloes, and 400 for GCs.

The orbits of the two spirals in any given run of the model are set to be initially in the xy plane by definition, and the distance between the centre of mass of the two spirals (r_{in}) is $6R_d$ (105 kpc). The pericentre distance (r_p) and the orbital eccentricity (e_p) are assumed to be free parameters which control the orbital angular momentum and energy of the merging galaxy. We show here the particular cases for $e_p = 1$ and $r_p = R_d$ (17.5 kpc), because the dynamics of halo formation do not depend strongly on these merger parameters. The spin of each spiral in a merging galaxy is specified by two angles θ_i and ϕ_i (in units of degrees), where the suffix i is used to identify each galaxy. Here, θ_i is the angle between the z axis and the vector of the angular momentum of the disc, and ϕ_i is the azimuthal angle measured from x axis to the projection of the angular momentum vector of the disc onto the xy plane. We specifically investigate the following three models with different disc inclinations with respect to the orbital plane: (a) a prograde-prograde model represented by "PP" with $\theta_1 = 0$, $\theta_2 = 30$, $\phi_1 = 0$, and $\phi_2 =$

0, (b) a prograde-retrograde ("PR") with $\theta_1 = 30$, $\theta_2 = 240$, $\phi_1 = 90$, and $\phi_2 = 0$, (c) a retrograde-retrograde ("RR") with $\theta_1 = 180$, $\theta_2 = 210$, $\phi_1 = 0$, and $\phi_2 = 0$. All calculations related to the above collisionless evolution have been carried out on the GRAPE board (Sugimoto et al. 1990) at the Astronomical Institute of Tohoku University.

2.2 MDFs of spirals

A key point of these simulations is to trace out what generates the MDF of the merger product halo. We thus assume that each stellar component within the progenitor spirals has its own characteristic MDF which does not change during a simulation of a galaxy merger. The initial MDFs for each of the stellar components (i.e., bulge, disc, halo, and GC) in a merger progenitor spiral are assumed to be different from one another, and are defined to mimic the observed ones in the Milky Way.

2.2.1 Disk

Recent photometric and spectroscopic observations of the Galactic stellar and gaseous components and gaseous components of external galaxies have demonstrated that disc galaxies have metallicities that depend on location within the disc, i.e., metallicity gradients (e.g., Zaritsky, Kennicutt, and Huchra 1994; Friel 1995). Considering these observations, we allocate metallicity to each disc star according to its initial position: at $r = R$, where r (R) is the projected distance (in units of kpc) from the center of the disc, the metallicity of the star is given as:

$$[m/H]_{r=R} = [m/H]_{d,r=0} + \alpha_d \times R. \quad (1)$$

We adopt two plausible values for the slope α_d : (a) -0.091 from Friel (1995) in which the Galactic stellar metallicity gradient is estimated from Galactic open clusters, and (b) -0.056 from Zaritsky et al. (1994) in which *gaseous* metallicity gradients of disc galaxies are estimated from HII regions of these. (It should be noted here that we do not have any observational results which have *directly* measured *stellar* metallicity gradients of external disc galaxies.) The models are labeled as "OC"-type (those with the Friel et al. gradient defined by open cluster metallicities) and "GAS"-type (those with the Zaritsky et al. gradient based on nebular and gaseous abundances). The value of the zeropoint $[m/H]_{d,r=0}$ is chosen such that the mean metallicity of a disc (represented by $[m/H]_d = -0.15$ for the fiducial model) can be different for different models.

We comment that the steeper "OC" slope might *a priori* be considered the preferable one, since it is based on the old- to intermediate-age stars which represent the bulk of the stars in the disc, and these stars are likely to be most relevant to mergers at the earlier epochs we are attempting to model here. By contrast, the "GAS" slope represents the youngest stars and present-day gas, which are a much smaller fraction of the disc mass. As will be seen below, α_d turns out to be perhaps the single most important parameter for understanding the outcome of the post-merger halo.

2.2.2 Bulge

The Galactic bulge is also observed to have a metallicity gradient (e.g., McWilliam & Rich 1994; Wyse et al. 1997; Frogel et al. 1999). Therefore in the models we assign the metallicity of a bulge star at $r = R$, where r (R) is the projected distance (in units of kpc) of the star from the center of the bulge, to be:

$$[m/H]_{b,r=R} = [m/H]_{b,r=0} + \alpha_b \times R. \quad (2)$$

We adopt the metallicity gradient from Frogel et al. (2000) in which the slope $\alpha_b = -0.43$. For the model with $M_b = 0.2$, we use $[m/H]_{b,r=0} = 0.034$. Since there is an observed relation between luminosity (L) and metallicity (Z) for spheroidal galaxies ($L \propto Z^{0.4}$; Mould 1984), we allocate a larger metallicity of $[m/H]_{b,r=0}$ to the model with a larger bulge. For example, the value of $[m/H]_{b,r=0}$ in the model with $M_b = 0.6$ is set to be 0.19.

2.2.3 Halo and GCs

There is no clear evidence of radial metallicity gradients in the Galactic halo stars or halo globular cluster system (e.g., Searle & Zinn 1978; Chiba & Yoshii 1998). We accordingly do not allocate a metallicity to each halo star (GC) based on its initial position. Instead, we assume that the halo stars (GCs) in a model have a Gaussian metallicity distribution with a mean of $[m/H]_h$ ($[m/H]_{gc}$) = -1.4 and dispersion of $\sigma([m/H]) = 0.3$ (and truncated at 4σ). The adopted value of $\sigma([m/H]) = 0.3$ has already been demonstrated to be a reasonable value in explaining the observed MDF of the Galactic stellar halo and GCs (e.g., Côté et al. 2000). We set the value of $[m/H]_{gc}$ to be -1.6 for all models.

Most large galaxies also have GCs which are more metal-rich and usually more concentrated to the galaxy center than the metal-poor halo clusters. In the Milky Way and M31, these more metal-rich clusters (which have a mean $[m/H] \simeq -0.5$ and higher overall rotation speed around the galaxy center) form about a quarter to a third of the whole GC population in both M31 and the Milky Way, and can plausibly be interpreted as a “bulge” component (see Perrett et al. 2002; Harris 2001; Minniti 1996). The MDF for the entire globular cluster system in these and many other large galaxies can usually be described as having a bimodal form (e.g. Larsen et al. 2001), often with a clear separation between the halo and bulge components. We do not explicitly include any bulge GCs in the simulations, because (as will be seen below) they behave similarly to the bulge stars during the merger, and at this stage we are interested primarily in the formation of the elliptical halo. We will discuss the GC results further in §3.2.

The MDFs for the various components of a progenitor spiral are given in Fig. 1 for the fiducial model (described in detail later) with the “OC” type metallicity gradient, $[m/H]_d = -0.15$, $M_b = 0.2$ (The Galactic bulge model), and $[m/H]_h = -1.4$.

2.3 Main points of analysis

For the NGC 5128 halo, MDFs have been obtained at projected distances of 8 kpc, 21 kpc, and 31 kpc from the galaxy center (HHP, HH00, HH02). The two outer-halo locations

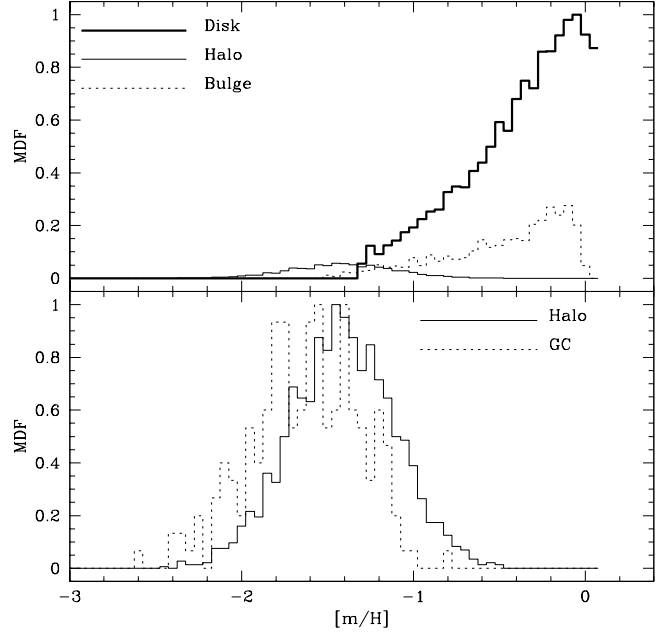


Figure 1. *Upper:* The MDFs of each of stellar component, disc (thick solid), halo (thin solid), and bulge (dotted) in a spiral galaxy for the fiducial model M1. “OC”-type metallicity gradient and a bulge mass ($M_b = 0.2$) are assumed in this model. *Lower:* The MDFs of the stellar halo (solid) and globular clusters (represented by GC, dotted) in a spiral galaxy for the fiducial model M1. Here $[m/H]_h = -1.4$ and $[m/H]_{gc} = -1.6$ are assumed in this model.

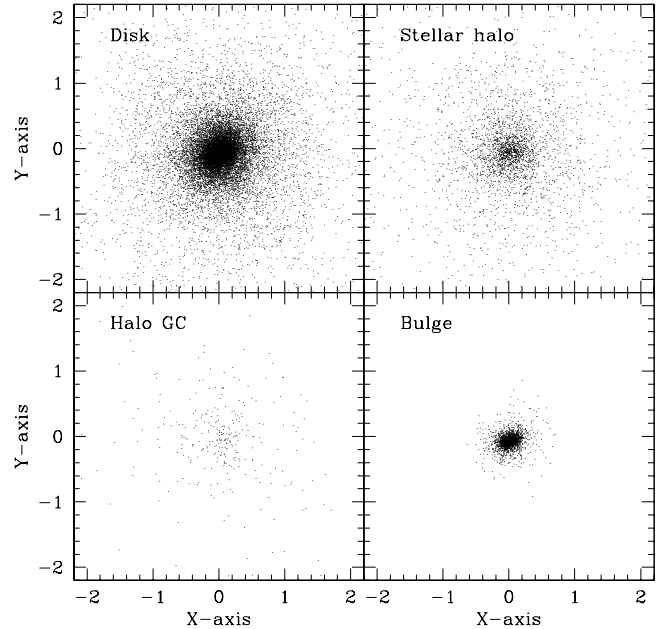


Figure 2. Final mass distribution of stellar components that are initially disc stars (upper left), halo ones (upper right), GCs (lower left), and bulge stars (lower right) in the elliptical galaxy formed by major merging in the fiducial model M1 at $T = 20$ in our units (2.8 Gyr). One frame measures 77 kpc on a side. Note that the halo region ($R > 0.5$) of this elliptical galaxy is dominated by disc stars.

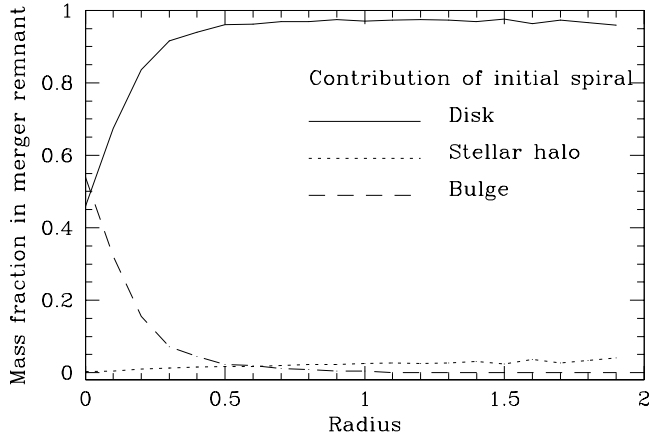


Figure 3. Radial dependence of mass fraction of each stellar component, disc (solid), halo (dotted), and bulge stars (dashed) in the merger remnant for the fiducial model M1. Note that more than 90 % of stars with $R > 0.5$ (regarded as “stellar halo” of the elliptical in the present study) are initially stars in the disc of the merger progenitor spirals.

(21 and 31 kpc) turned out to give identical results for the MDF. For comparison with the models, we investigate the model MDFs of two halo regions which correspond closely with these inner and outer regions, one at $0.5 < R \leq 1.0$ (referred to as “inner halo”) and the other at $1.0 < R \leq 2.0$ (“outer halo”) in each merger model. The simulated MDF of the “inner halo” and that of the “outer halo” are compared with the observed MDF derived for the 8 kpc field and with that derived for the combined 21 and 31 kpc fields. Although we investigated ~ 20 models, we here present only the results of the models which are not obviously inconsistent with observational results. That is, we attempt to outline the range of model parameter space which leads to realistic results. For example, our simulations have shown that, if the halo mass fraction of the merger progenitor spirals is greater than 0.2, the resultant MDF has far too many metal-poor stars to agree with the observed MDF. Equally, if the initial disc’s mean metallicity in a merger is much larger than $[m/H] = 0.0$, the peak value of the resultant MDF is too metal-rich to be consistent with observations. We will not show the results of these obviously inconsistent models here but, rather, we present the results of the more realistic models in which the mean disc metallicity ($[m/H]_d$) is equal to -0.15 and 0.0 , and in which the halo mass fraction is no more than 0.2.

Below, we describe the results of 10 models and in Table 1 summarize their input parameters: model number (column 1), bulge mass fraction M_b (column 2), metallicity gradient type (3), mean metallicity of disc in $[m/H]_d$ (4), orbital type of galaxy merging (5), halo mass fraction f_h (6), and initial halo mean metallicity $[m/H]_h$ (7). For convenience we refer to the model M1 as the *fiducial model*. It shows typical behavior of stellar halo formation in major merging and its MDF is reasonably consistent with the observations of the NGC 5128 stellar halo. Accordingly we describe mainly the results of this model in the following sections. The MDFs of this model for each component (disc, bulge, halo, and GCs) are summarized in Table 1. The metallicity gradient types “OC” and “GAS” in the third column

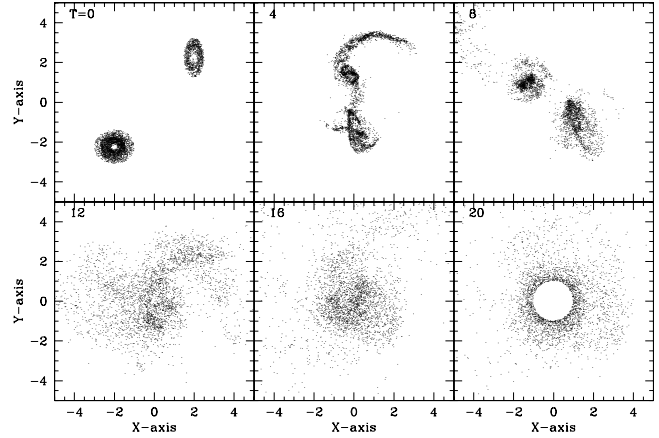


Figure 4. Morphological evolution of disc stars that become halo stars with $R > 1$ (where R is the projected distance from the center of the merger in our units) at $T = 20$ (2.8 Gyr) in the fiducial merger model M1 projected onto the x - y plane. The scale is given in our units, and accordingly each frame measures 175 kpc on a side. Note that the outer halo stars of the merger remnant are initially located in the outer part of the progenitor discs. Note also that tidal stripping (or angular momentum redistribution) of disc stars during major galaxy merging is a key physical process of the stellar halo formation in the elliptical galaxy. The six boxes show this evolution at times of $T=0, 4, 8, 12, 16$, and 20.

represent the two choices for disc metallicity gradient described above. Orbital type labels “PP”, “PR” and “RR” represent a nearly prograde-prograde orbital configuration, a prograde-retrograde one, and a nearly retrograde-retrograde one. The structural properties of merger remnants are briefly summarized in Appendix A.

3 RESULTS

3.1 Dynamics of stellar halo formation and MDFs of ellipticals

Figs. 2 and 3 summarize the final mass distributions of the stellar components that are initially within discs, haloes, and bulges of the merger progenitor spirals for the fiducial major merger model M1. Since the bulges initially have more compact configurations than the discs, only a small fraction of bulge stars are tidally stripped to form the inner stellar halo with $0.5 < R \leq 1.0$ of the merger remnant, where R is the radius from the center of the developed elliptical galaxy in units of R_d . The stars in the discs, on the other hand, are very efficiently stripped owing to the strong tidal field of major merging (or by angular momentum redistribution during merging) so that they end up in both the inner and outer halo ($1.0 < R \leq 2.0$) of the elliptical galaxy. Although the initial stellar haloes of the spirals are also stripped (or ‘puffed up’) efficiently to form the inner and the outer stellar haloes, the stellar halo of the resulting elliptical is dominated by the stars that were initially within the progenitor discs; about 95% of the elliptical halo comes from the initial disc stars at $1 < R$ (For comparison, the outer parts of the spirals with $1 < R \leq 2$ are by definition dominated *only* by their metal-poor halo stars). These results imply that major mergers can efficiently populate the stellar haloes of their

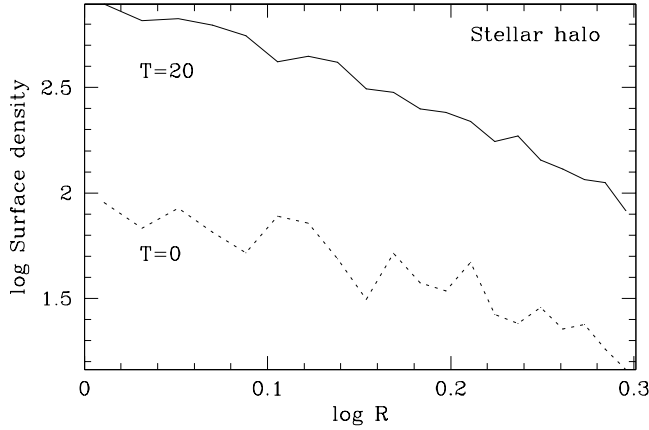


Figure 5. Radial distribution of the surface (number) density of stars located in the halo region of the merger model M1 at $T = 20$ (solid) and those in the halo region of the progenitor spiral at $T = 0$ (dotted). Here the results are given for the “outer” halo region ($1 < R \leq 2$). The scale is given in our units, and accordingly the outer halo region corresponds to $17.5 < R \leq 35.0$ kpc.

product elliptical galaxies by disc stars from within their progenitor spirals.

We note also from Fig. 4 that the (outer) stellar halo of the elliptical galaxy comes from the outer part of the merger progenitor disc, because the tidal stripping (or angular momentum redistribution) is more efficient for the outer part of the disc than for the inner part. Furthermore, Fig. 4 shows that, although the violent dynamical relaxation of major merging results in strong mixing of stars of the two discs, we can clearly see the inhomogeneous distribution of halo stars at $2 < R$ (e.g., the upper right part of the halo appears to be denser than the lower left). This implies that if we can observe *the global* stellar halo or surface intensity distribution of an elliptical galaxy, it may show a certain degree of inhomogeneity.

As is shown in Fig. 5, the surface density of the merger halo is greater by roughly 2 orders of magnitude at a given radius than the initial spiral halo owing to the stripped disc stars. This result suggests that the surface brightness of stellar haloes in elliptical galaxies will be systematically higher than for haloes in spiral galaxies if most ellipticals are formed by major merging. However, the slope of the halo light distribution does not change significantly compared with that of the initial spiral halo.

A significant result of the halo formation by stripping of disc stars is that the MDF of the stellar halo of the elliptical galaxy becomes remarkably different from that of the progenitor spirals. We show this, and the comparison with the data, in Figures 6 and 7. By comparing Fig. 1 and Fig. 6, we also note that the difference in MDFs between the halo and the disc (spheroidal) components in this model becomes much smaller after merging. This implies that the MDFs of the stellar haloes in elliptical galaxies are less different from those of the main spheroidal bodies than they are in spirals.

As is shown in the lower panel of Fig. 6, the stellar halo of the emergent E galaxy is a genuine composite population in this formation scheme. The relatively metal-rich part which is the vast majority ($[\text{m}/\text{H}] > -1$) come from the progenitor discs, whereas the thin metal-poor part comes from

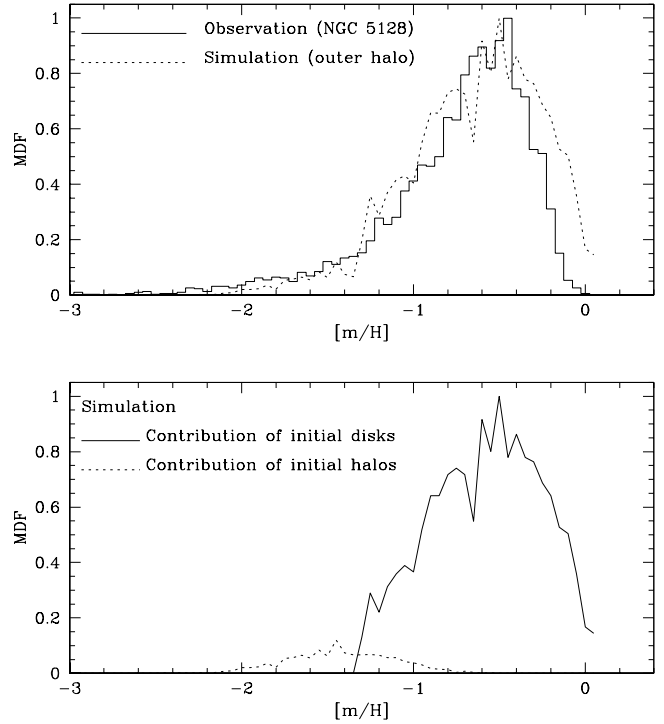


Figure 6. *Upper:* MDFs derived for observations (solid) and the simulation of model M1 (dotted). The MDF for observations is constructed from halo stars with the projected distance of 21 and 31 kpc in NGC 5128 halo fields. The MDF for the simulation is constructed from the simulated stars with $1 < R \leq 2$ ($17.5 \text{ kpc} < R \leq 35 \text{ kpc}$), where R is the distance of a star from the center of the merger remnant. Note that the simulated MDF shows a peak around $[\text{m}/\text{H}] \sim -0.4$, which is similar to the observed peak. *Lower:* MDFs for stars that are initially disc stars (solid) and halo ones (dotted) in the simulation of model M1. These MDFs are also estimated for the outer halo region with $1 < R \leq 2$. Bulge stars do not contribute to the MDF in this outer halo at all.

the progenitor haloes. A very small fraction at the metal-rich end is from the original bulges.

Fig. 7, showing the inner halo ($0.5 < R \leq 1.0$) of the elliptical galaxy, has an MDF which is shifted even further to the metal-rich end, with a broad peak at $[\text{m}/\text{H}] \sim -0.4$ and an extension to well above Solar metallicity, and an even sparser low-metallicity tail than the outer halo. Here, a higher fraction of the stars are from further in within the progenitor discs ($\sim 97\%$), as well as from the initial bulges ($\sim 2\%$). The simulated MDF is not as broad as the observed inner halo MDF and, in particular, does not extend as far into the metal-rich regime. This may be significant, particularly since the observed data are likely to be more incomplete for the reddest stars (HH02). Thus the principal driver of the observed metallicity gradient in the resulting E galaxy halo is the presence of the initial metallicity gradients in the disc. Fig. 8 demonstrates that the MDF in the very outer part of the halo ($R > 2$, corresponding to $R > 35 \text{ kpc}$) shows a much wider peak around $-1 < [\text{m}/\text{H}] < -0.4$ and a larger fraction of metal-poor ($[\text{m}/\text{H}] < -1.0$) stars compared with the MDFs for the inner and the outer haloes. This is mainly because the very outer halo with $R > 2$ consists of more metal-poor stars coming from the extreme outer parts of the merging discs. The predicted difference in the MDFs

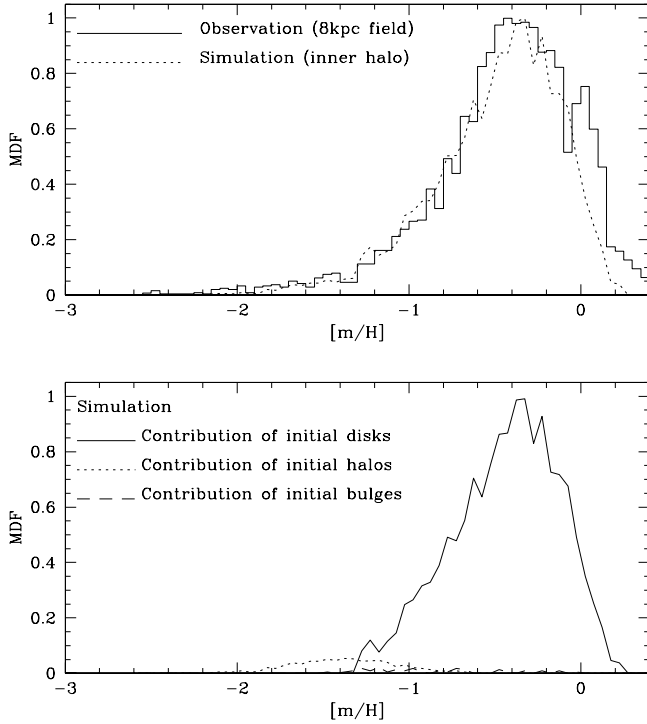


Figure 7. The same as the Figure 6 but for the inner halo region with $0.5 < R \leq 1.0$. The MDF for observations is constructed from halo stars with the projected distance of 8 kpc in NGC 5128 halo fields. In the lower panel, MDFs for stars that are initially disc stars (solid) and halo ones (dotted), and bulge ones (dashed) are plotted.

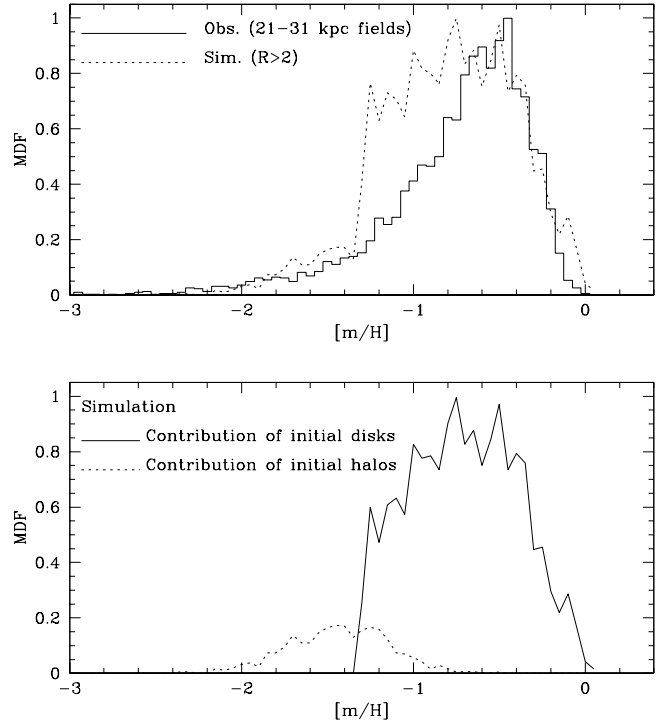


Figure 8. The same as the Figure 6 but for the very outer halo regions with $2.0 < R$. The MDF for observations is constructed from halo stars with the projected distance of 21 and 31 kpc in NGC 5128 halo fields.

between the outermost halo ($2 < R$) and the already observed inner and outer haloes (i.e., $0.5 < R \leq 1.0$ and $1.0 < R \leq 2.0$) can be tested by future observations on the MDF of the NGC 5128 stellar halo at projected distances of larger than 30 kpc.

In Fig. 9, we show the dependence of mean metallicity on galactocentric distance for the merged elliptical and the initial spirals. The *outer* stellar halo of the model elliptical ($1 < R \leq 2$) does not show any important metallicity gradient, though its progenitor *discs* have negative metallicity gradients. This is mainly because violent dynamical relaxation during galaxy merging can cause efficient mixing of stellar populations (with different metallicity) initially located in different regions of the discs, and this almost completely smoothes out the initial disc's metallicity gradient. (It should be noted here that if we observed the gradient *throughout* the elliptical, we can still see the negative gradient, which becomes steeper farther in to the center.) Fig. 9 also demonstrates, as indicated above, that the mean metallicity of the stellar halo of the elliptical is much higher (\sim a factor of 6) than that in the progenitor spiral *at all points* in the outer halo regions. This is remarkably consistent with the HST data for the NGC 5128 fields at 21 kpc and 31 kpc whose MDFs are virtually indistinguishable (HH00). We suggest that the near-zero metallicity gradient of the outer stellar halo is an observational test which can assess the validity of the merger scenario of elliptical galaxy formation.

In Fig. 10 we show the distribution of the halo stars on the V_y -[m/H] diagram (radial velocity vs. metallicity) for the

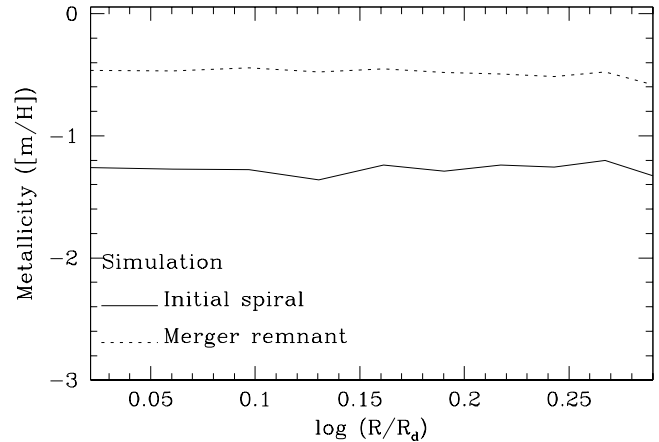


Figure 9. Metallicity gradient of the stellar halo with $1 < R \leq 2$ in the initial spiral (solid) and the merger remnant (dotted) for the model M1. Note that values of $\log (R/R_d) = 0.08$ and 0.25 correspond to the approximate locations of the observed 21kpc and 31 kpc fields.

progenitor spirals and the elliptical. Only the elliptical halo contains stars with both high projected (radial) velocity ($V_y \sim 2$ in our units, corresponding to $\sim 280 \text{ km s}^{-1}$) and high metallicity ($[m/H] > -0.6$). Some fraction of these outer halo stars with rather high projected velocity also have large tangential velocities and thus high angular momentum with respect to the elliptical. The origin of these halo stars with high angular momentum is closely associated with angular momentum transfer, from inside to outside, during major

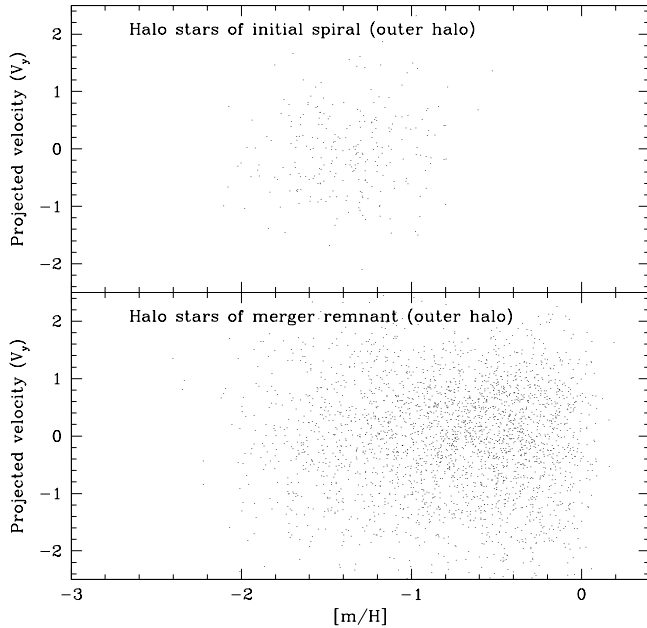


Figure 10. Distribution of halo stars with $1 < R \leq 2$ (outer halo) on V_y -[m/H] diagram for the merger progenitor spiral (upper) and the merger remnant (lower) in the model M1. V_y here represents the velocity of a star projected onto y -axis of the simulation. Note that there are a larger number of halo stars with $[m/H] > -0.6$ and the absolute magnitude of V_y larger than 1.8 (250 km s^{-1}) only in the merger remnant. A physical interpretation of this is given in the text.

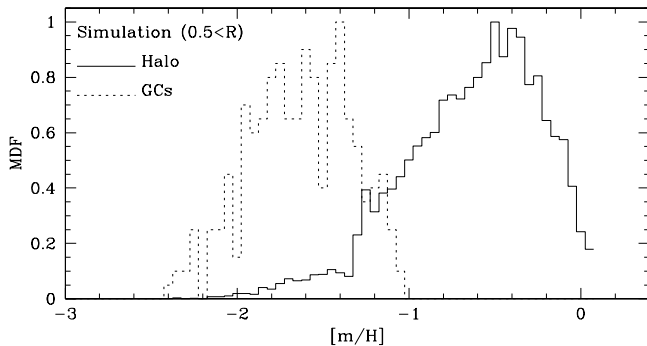


Figure 11. MDFs of halo stars (solid) and halo GCs (dotted) in the merger remnant of the model M1 at $T = 20$. The MDFs are constructed from the stellar components with $0.5 < R$ (i.e., both the inner and the outer stellar components). Note that there is a clear difference in MDFs between the halo and the GC. This clear difference is not seen in the initial spiral’s MDF (See Fig. 1), which suggests that dynamical processes of galaxy merging cause such a remarkable difference in the MDFs between the halo and the GCs in the model M1.

galaxy merging; orbital angular momentum of the merging spirals is converted into the intrinsic angular momentum of such outer halo stars. Based on kinematics and spatial distribution of the planetary nebula (PN) system in NGC 5128, Hui et al. (1995) found a possible evidence of the PN’s rotation increasing with radius and discussed the origin of this elliptical galaxy. Additional new velocity analyses are given by Peng et al. (2002). Although the necessary spectroscopic data to obtain kinematical properties of individual halo stars

in NGC 5128 are beyond current observational capabilities, the results in Fig. 10 suggest that, future such observations may find a larger fraction of relatively metal-rich outer-halo stars with high angular momentum in NGC 5128.

3.2 Globular clusters

By comparing Fig. 1 with Fig. 11, we can clearly see that the difference between the GC and field-star MDFs in this merger model becomes much more conspicuous after elliptical galaxy formation. This is essentially because the GCs start out as part of a “hot”, pressure-supported component of the spiral haloes and so behave differently from the disc stars during the merger. The MDF of the halo clusters thus does not change markedly during merging, whereas that of the halo can be dramatically changed owing to the addition of large numbers of stripped disc stars. In the product elliptical, we therefore end up with metal-poor clusters embedded in a moderately metal-rich and massive halo.

This dynamically constructed difference in MDFs would not be changed if we were to include gas and merger-induced formation of metal-rich GCs, since numerical simulations have already demonstrated that these would mostly be located in the central region of the merger remnant and therefore would not contribute to the MDF of GCs in the outer halo region (Bekki et al. 2002). In addition, the “bulge” GCs which were already present in the progenitor spirals (such as are present in both the Milky Way and M31) are more concentrated to their parent galaxy centers and would stay in the inner regions along with the bulge stars. The significant difference in MDFs between the halo stars and the GCs that we note in the M1 simulation has been actually observed for M31 (Durrell et al. 2001) and NGC 5128 (HHP, HH01, HH02), both of which have large central spheroidal components. A mean offset in integrated color (and by hypothesis metallicity) between GCs and field stars is also classically observed in many giant ellipticals (e.g. Harris 1991, Brodie & Huchra 1991). It has frequently been suggested that the redder, more metal-rich clusters are similar to the bulk of the field halo and bulge stars, while the bluer, more metal-poor ones have earlier and different origins, such as within spiral haloes or dwarf galaxies (e.g. Larsen et al. 2001; Forbes, Brodie, & Grillmair 1997; Geisler, Lee, & Kim 1996; Côté, Marzke, & West 1998). The Milky Way, an Sbc-type spiral with only a small bulge, is not observed to have such a difference between halo stars and clusters. We therefore suggest that the observed difference in MDFs between stellar haloes and GCs in elliptical galaxies or early-type spirals with big bulges is consistent with the view that their large spheroidal components were formed by past major merger events. We discuss this point further in §4.

3.3 Parameter dependences

Although the models M1 – M10 resemble each other in their dynamics of stellar halo formation and the peak value of the MDFs of the resulting stellar haloes, the shapes of the MDFs depend on the progenitor disc metallicity gradient, bulge-to-disc-ratio, and the mass fraction and the MDFs of the initial haloes. In Fig. 12, we illustrate these effects:

- (i) The MDFs show a larger fraction of metal-rich (-0.4

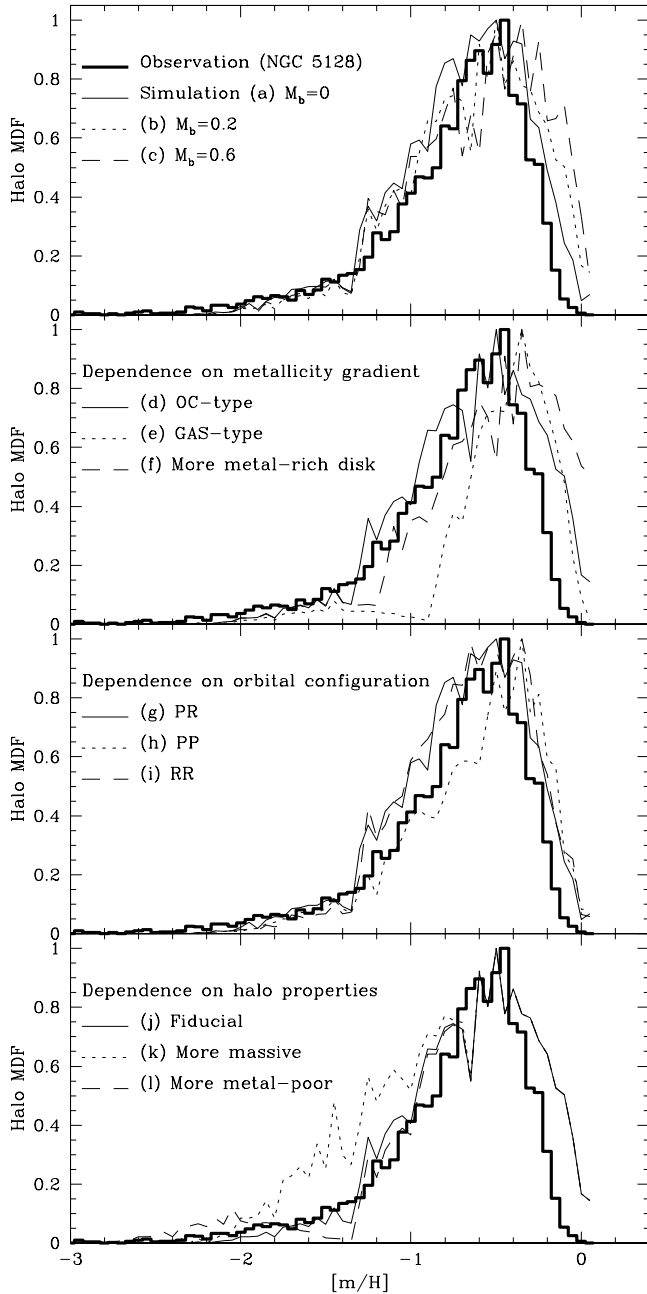


Figure 12. Dependence of the simulated MDFs on the initial mass fraction of bulge (top), the MDFs of the merger progenitor discs (second from the top), orbital configurations of major merging (second from the bottom), and MDFs of the stellar haloes of the merger progenitor spirals (bottom). For comparison, the MDF observed for the stellar halo regions with projected distances of 21 and 31 kpc in NGC 5128 (HHP, HH00, and HH02) is given by a thick solid line in each panel. The results are given for (a) the model with $M_b = 0$ (solid, M3), (b) $M_b = 0.2$ (dotted, M1), (c) $M_b = 0.6$ (dashed, M2), (d) “OC”-type metallicity gradient (solid, M1), (e) “Gas”-type one (dotted, M4), (f) more metal-rich disc with $[m/H]_d = 0$ (dashed, M5), (g) “PR” (prograde-retrograde) orbital configuration (solid, M6), (h) “PP” (prograde-prograde) orbital configuration (dotted, M7), (i) “RR” (retrograde-retrograde) orbital configuration (dashed, M8), (j) the fiducial set of parameters (solid, M1), (k) more massive ($f_h = 0.2$) stellar halo (dotted, M9), and (l) more metal-poor ($[m/H]_h = -2$) stellar halo (dashed, M10).

$\leq [m/H] \leq 0$) halo stars in the model with the larger bulge-to-disc-ratio ($M2$, $M_b = 0.6$). This is because more of the metal-rich bulge stars can be more efficiently stripped into the stellar halo owing to its larger extension of the bulge in the model with the larger bulge-to-disc-ratio. The MDF derived in the model with the smaller bulge-to-disc-ratio ($M3$, $M_b = 0$) seems to be more similar to the observed MDF of the NGC 5128 stellar halo, although we stress (see HH02) that the data may be somewhat incomplete at the highest metallicities. Nevertheless, the current comparisons would allow NGC 5128 to be formed by major merging between later-type spirals.

(ii) The stellar halo in the model ($M4$, GAS-type) which was generated from progenitor spirals with the shallower disc metallicity gradients (gaseous nebulae abundances; Zaritsky et al. 1994) can not match the observations. Such models predict far too few stars in the intermediate metallicity range ($-1.4 \leq [m/H] \leq -0.6$). The input discs with steeper metallicity gradients (OC-type) produce a much closer match to the observations. The opposite problem is presented by model $M5$, which has a larger initial mean disc metallicity; this model ends up predicting far too many halo stars for $[m/H] \geq -0.2$. These results are the most prominent ones of our investigation, and indicate that the detailed shape of the observed MDF in NGC 5128 can provide information on the mean metallicity and disc gradients in the merger progenitor spirals (and thus, possibly, on their luminosity due to the observed color-magnitude relation for disc galaxies).

(iii) The shapes of the MDFs of stellar haloes of elliptical galaxies formed by major merging do not depend strongly on the orbital configurations of the merging ($M6$, 7, and 8). This probably reflects the fact that the physical processes of violent relation and angular momentum redistribution do not so strongly depend on the orbital parameters of major merging. The PP model shows a slightly higher peak value of the MDF, because a larger amount of disc stars can be stripped owing to more efficient angular momentum redistribution process in this model.

(iv) Lastly, the stellar haloes in the progenitor spirals exert noticeable effects on the stellar halo of the merger remnant at the low-metallicity end ($[m/H] \leq -1.2$). The model $M9$ with the larger initial mass fraction of the spiral’s halo (20 %) produces too many halo stars at $-1.8 \leq [m/H] \leq -1$ and is not consistent with the observations. The model haloes with mass fractions of 5% yield much closer matches to the data. In short, the model comparisons appear to rule out progenitor spirals with very massive, metal-poor haloes.

4 A NEW CONSTRAINT ON ELLIPTICAL GALAXY FORMATION

Although the observed tight color-magnitude relation of elliptical galaxies has been considered to suggest that elliptical galaxies are old, coeval and homogeneous systems passively evolving after the single initial burst of star formation associated with dissipative galaxy formation (e.g., Bower, Lucey, & Ellis 1992), a growing number of recent observational results suggest that elliptical galaxies exhibit a great variety of star formation history (e.g., Worthey, Trager, & Faber 1996). The observed narrowness of the fundamental plane of elliptical galaxies implies a rather smaller range of per-

mitted dynamical state of the galaxies (Djorgovski & Davis 1987; Dressler et al. 1987). However, the morphological dichotomy between boxy-disk elliptical galaxies (Kormendy & Bender 1996) and departures of the projected density profiles from the de Vaucouleurs $R^{1/4}$ law (Caon, Capaccioli, & D’Onofrio 1993) show a great variety of major stellar orbit families within the galaxies. Elliptical galaxies thus show both diversity and uniformity in their chemical, photometric and dynamical properties which impose valuable constraints on any theoretical models of elliptical galaxy formation.

The present study has demonstrated that, irrespective of bulge-to-disc-ratio and MDF of progenitor spirals, elliptical galaxies formed by major merging show the tendency for stellar haloes to be populated predominantly by moderately metal-rich stars in the range $-1 < [\text{m}/\text{H}] < 0$ which were originally in the spiral discs. Classical monolithic collapse scenarios (e.g., Larson 1976; Carlberg 1984) which have shown strong negative metallicity gradients (i.e., more metal-poor in the outer part of a giant elliptical) are less likely to yield the moderately metal-rich populations in the outer halo regions that we see in our test case of NGC 5128. Therefore, if future systematic observations on MDFs of elliptical galaxies confirm the above generic trend in their halo MDFs, it would provide evidence more consistent with major merging as a promising scenario of elliptical galaxy formation.

Spiral galaxies exhibit a color-magnitude (CM) relation with a slope steeper than those of elliptical galaxies (de Grijs & Peletier 1999). If the CM relation is due mostly to metallicity vs. luminosity (i.e., no significant age effects on integrated colors), then more luminous spirals should be more metal-rich. The present numerical studies have demonstrated that the mean halo metallicity of an elliptical depends strongly on the mean metallicity of the merger progenitor discs, and furthermore that the mass fraction of stellar haloes is not different between different merger models. These observational and theoretical results lead to the prediction that if the majority of E galaxies were formed by major mergers (that is, a single merger event between roughly equal progenitors), there should be a strong correlation between the color (mean metallicity) of the stellar halo and the absolute magnitude of its host elliptical galaxy: the more luminous (redder) elliptical should show redder halo colors. In this picture, if there are very luminous ellipticals with rather metal-poor haloes that violate this correlation, they would have been formed by a longer series of mergers from smaller, more metal-poor progenitors or perhaps by accretion as in Côté et al. (1998, 2002).

4.1 Origin of the M31 stellar halo

Since Mould & Kristian (1986) first resolved clearly the brightest RGB and AGB stars in the M31 halo, many observational studies of its MDF have been done (e.g., Pritchet & van den Bergh 1988; Christian & Heasley 1991; Davidge 1993; Durrell, Harris, & Pritchet 1994; Couture et al. 1995; Holland, Fahlman, & Richer 1996; Rich, Mighell & Neil 1996; Reitzel, Guhathakurta, & Gould 1998; Reitzel & Guhathakurta 2001; Durrell, Harris, & Pritchet 2001). One of the most remarkable results of these studies is that the derived MDF of the M31 halo is very different from that of the Milky Way halo. All the studies listed above find that

the M31 halo is dominated by moderately high-metallicity ($[\text{m}/\text{H}] \sim -0.5$) populations at a very similar level to what we find in NGC 5128. Durrell, Harris, & Pritchet (2001) point out that the bulk of the M31 halo stars are much less likely to come from dwarf galaxy populations, just as for NGC 5128. Côté et al. (2000) demonstrated that if the M31 halo was formed by dissipationless merging of numerous subgalactic clumps with a luminosity (L) function of slope $dn/dL \propto L^{-1.8}$, the observed MDF could be reproduced. However, it is not clear *a priori* why the MDFs of the Milky Way and M31 should be so different in the same Local Group environment with the plausible assumption that the surrounding pregalactic population of clumps would be similar for both. Ibata et al. (2001) suggest that the bulk of the M31 halo may have arisen from a single event, namely cannibalization of stars from the similarly metal-rich satellite M32.

We here propose that the origin of the M31 stellar halo can be closely associated with M31’s bulge formation via major merging of two discs at an early epoch (see also Freeman 1999). In this scenario, the metal-rich halo stars were initially within the outer parts of the merger progenitor spirals and tidally stripped during the M31’s bulge formation. This merger scenario can give a plausible explanation as to why the MDFs in the haloes of M31 and NGC 5128 resemble each other so strongly (Harris & Harris 2001). If the observed difference in the metallicity of the dominant metal-rich population between these two can reflect the difference in mean metallicity of merger progenitor spirals between these two, we can estimate the luminosity difference between the progenitor spiral of M31’s bulge and that of NGC 5128. The metallicity of the dominant halo population is $[\text{m}/\text{H}] \sim -0.5$ for M31 (Durrell, Harris, & Pritchet 2001). and -0.4 for NGC 5128 (HHP; HH00, 02). By using the observed luminosity-metallicity relation $Z \propto L^{0.4}$ (Mould 1984), we can expect that the possible luminosity difference of merger progenitor spirals between these two big spheroidal components is a factor of ~ 2 . This difference is appreciably smaller than the observed luminosity difference (a factor of ~ 4) between M31’s bulge with $L_V \sim 1.1 \times 10^{10} L_\odot$ corresponding to about 40 % of total stellar light of M31 (van den Bergh 2000) and NGC 5128 with $L_V \sim 4.7 \times 10^{10} L_\odot$ (Hui et al. 1995).

Freeman (1999) suggested that the big M31 bulge could be formed by a past merger event on the basis of M31’s halo structural properties. He also pointed out that if M31’s bulge was formed by merging, its *outer* stellar halo components should show significant rotation owing to efficient angular momentum transfer during merging. Our present simulations have confirmed that the outer stellar halo components clearly show rotation after major merging. We note that Perrett et al. (2002) have indeed found a strong rotation signature for both types of globular clusters in the M31 halo (160 km s^{-1} for the metal-rich population, 130 km s^{-1} for the metal-poor population), extending outward to $\sim 15 - 20 \text{ kpc}$.

Big spheroidal bulges (like M31’s) are suggested to be physically different from box- and peanut-shaped bulges in spirals (e.g., Wyse et al 1997 and references therein): Spheroidal bulges are “true” bulges similar to giant ellipticals whereas the box- and peanut-shaped bulges are edge-on bars formed through dynamical instability of discs

(e.g., Combes & Sanders 1981). We suggest that if “true” spheroidal bulges are formed by merging (rather than disc instability), spirals with such big bulges are more likely to show halo MDFs similar to that of M31 rather than to that of the Milky Way. It would be an interesting future study to correlate the MDFs of stellar haloes with bulge shapes in different Hubble types of galaxies.

4.2 Discussion and Remaining Problems

We close by briefly mentioning alternate models of halo formation applicable to NGC 5128 and other ellipticals, along with difficulties still faced by most interpretations.

E galaxies may also form by longer series of mergers (accretion) of smaller subgalactic clumps. The dissipationless accretion of dwarf galaxies with appropriate chosen luminosity functions can be also responsible for MDFs with relatively metal-rich peaks (e.g., Côté et al 1998, 2000, 2002). As also noted earlier, Beasley et al. (2002a,b) take the alternate route of hierarchical merging of pregalactic gas clouds to model the NGC 5128 MDF, with first-order matches possible in a wide variety of circumstances. Without repeating the extensive analysis in these papers, we note only that their work demonstrates that a unique physical interpretation for the observed MDFs may still not be in hand. Eventually, all the observational parameters including kinematics and halo/bulge structures as well as MDFs must be brought to bear on the question.

There are, however, two interesting interpretive problems which the globular cluster populations confront us with. First is the sheer size of the cluster population in NGC 5128. Coincidentally, the luminosity of NGC 5128 ($M_V \simeq -22.0$) is similar to what we would get if we simply combined two galaxies like M31, or M31 plus the Milky Way (Pritchet & van den Bergh 1999). Thus a simple merger of the two would give an elliptical of about the same size as NGC 5128 and with $\sim 600 - 800$ clusters. A GC population of that size is two to three times smaller than the $\sim 1500 - 2000$ globular clusters that are in NGC 5128 (G.Harris et al. 1984). That is, NGC 5128 has a GC specific frequency significantly higher than normal spiral galaxies. Contrary to many comments in the literature, this classic “specific frequency problem” cannot be solved by invoking the presence of gas and then forming large numbers of clusters during the merger. This is because field stars will also form from the gas, and the ratio of field stars to GCs will stay at much the same level. See the discussion of Harris (2001), who notes that to produce noticeable changes in the specific frequency, it is necessary to have *both* extremely large amounts of gas *and* extremely high cluster formation efficiency. Under such conditions, we would no longer be talking about a simple disc/disc merger but rather an earlier epoch of primary galaxy formation from hierarchical merging of gas clouds.

A second concern relates to the spatial distributions of the GCs in the metal-poor and metal-rich subgroups that many or most giant ellipticals contain. The GCs in the metal-rich mode are not found only in the bulge region as noted above, but also extend outward far into the halo in significant numbers (e.g., G.Harris et al. 1992; Lee & Geisler 1993; Geisler, Lee, & Kim 1997). Such metal-rich clusters are also present in the outer halo of M31 (Perrett et al.

2002). Within the context of the merger scenario we have tested here, it is not clear how these metal-rich, outer-halo clusters arise. Clusters formed from appropriately metal-rich gas during the merger are likely to build up in the central regions and add to the bulge population. Metal-rich globular clusters that are *already* distributed widely throughout the discs or haloes of the progenitor spirals would end up populating the halo of the emergent elliptical. Such clusters are present to some extent in M31, but not in the Milky Way. In summary, it is still difficult for any one model to correctly predict the total ensemble of features of the giant ellipticals, which may have formed by a combination of routes.

5 CONCLUSIONS

We have numerically investigated MDFs of stellar haloes of elliptical galaxies formed by major merging in order to elucidate the origin of the observed MDF of NGC 5128. We mainly investigated the MDF of halo stars with $R > R_d$ (where R and R_d are the radius from the center of a merger remnant and the initial size of the merger progenitor spiral) in the merger remnant for several models with different physical parameters of the progenitor spirals. Our numerical study clearly demonstrates the importance of *dynamical processes of galaxy merging* (i.e., tidal stripping of metal-poor disc stars) in determining MDFs of stellar haloes of elliptical galaxies. We summarize our principal results as follows.

(1) The stellar halo of an elliptical galaxy formed by major merging is predominantly populated by moderately metal-rich stars with $[m/H] \sim -0.4$, which come from the outer parts of the discs of the merging spirals. Furthermore, the fraction of metal-poor stars with $[m/H] < -1.0$ in the halo is very small ($\sim 17\%$). The MDF of the merger remnant does not show a strong radial dependence for $0.5 < R < 2.0$ (in our units). These results are broadly consistent with recent *HST* observations on MDFs of the stellar halo of NGC 5128.

(2) Irrespective of the physical parameters of merger progenitor discs, the MDFs of stellar haloes of merger remnants show both the dominant moderately metal-rich populations and the minor metal-poor ones. Thus future systematic observations on MDFs of elliptical galaxies can assess the relative importance of major galaxy merging in the formation of elliptical galaxies by confirming the above generic trend of MDFs.

(3) The MDFs of elliptical galaxies formed by major merging depend strongly on the initial MDFs of merger progenitor discs, because halo stars are dominated by those which are initially in the outer part of the discs and tidally stripped during merging.

(4) MDFs of stellar haloes do not depend so strongly on the MDFs of the progenitor spiral bulges, essentially because bulge stars are not be tidally stripped so efficiently during merging owing to bulge’s compact configuration. However, the shapes of MDFs of a merger remnant at $-0.2 \leq [m/H] \leq 0$ can be affected by the bulge-to-disc-ratio of the merger progenitor spiral.

(5) The shape of the halo MDF of a merger remnant at $[m/H] \leq -1.0$ depends on the mass fraction and the mean metallicity of the progenitor spiral’s halo. Therefore the observed shape of the halo MDF at $[m/H] \leq -1.0$ in NGC

5128 can give some constraints on the stellar populations of the progenitor spiral's stellar halo.

(6) The observed similarity in MDFs of stellar haloes between M31 and NGC 5128 can be naturally explained, if the M31 bulge was also formed by major merging between two spirals with the masses (a factor of 2 – 4) smaller than those that are assumed to merge to form NGC 5128 in the present study. The observed markable difference in MDFs between stellar haloes and GCs for NGC 5128 and M31 can be also explained by the merger scenario.

(7) Our simulations predict that if most elliptical galaxies are formed by major merging, the photometric properties (e.g., colors and magnitudes) of a stellar halo in an elliptical galaxy can correlate with those of the galaxy (i.e., redder Es have redder stellar haloes). Also our study predicts that there can be CM relations in stellar haloes of elliptical galaxies.

6 ACKNOWLEDGMENT

K. B. acknowledges the financial support of the Australian Research Council throughout the course of this work. W.E.H. and G.L.H.H. acknowledge financial support from the Natural Sciences and Engineering Research Council (NSERC) of Canada and the hospitality and support at Mt Stromlo Observatory (RSAA/ANU) during research leaves when this paper was written.

REFERENCES

- Beasley, M.A., Baugh, M.A., Forbes, D.A., Sharples, R.M., and Frenk, C.S. 2002a, *MNRAS*, 333, 383
- Beasley, M.A., Harris, W.E., Harris, G.L.H., and Forbes, D.A. 2002b, *MNRAS*, accepted (astro-ph/0211586)
- Bekki, K., Beasley, M.A., Forbes, D.A., & Couch, W. J., 2002, accepted in *MNRAS*
- Bower, R. G., Lucey, J. R., & Ellis, R. S. 1992, *MNRAS*, 254, 601
- Brodie, J. P., & Huchra, J. P. 1991, 379, 157
- Caon, N., Capaccioli, M., & D'onofo, M. 1993, *MNRAS*, 265, 1013
- Carlberg, R. G. 1984, *ApJ*, 286, 416
- Chiba, M., & Yoshii, Y. 1998, *AJ*, 115, 168
- Christian, C. A., & Heasley, J. N. 1986, *ApJ*, 303, 216
- Combes, F.; Sanders, R. H. 1981, *A&A*, 96, 164
- Côte, P., Marzke, R. O., West, M. J., 1998, *ApJ*, 501, 554
- Côte, P., Marzke, R. O., West, M. J., & Minniti, D. 2000, *ApJ*, 533, 869
- Côte, P., West, M. J., Marzke, R. O. 2002, *ApJ*, 567, 853
- Couture, J., Racine, R., Harris, W. E., & Holland, S. 1995, *AJ*, 109, 2050
- Davidge, T. J. 1993, *ApJ*, 409, 190
- de Grijs, R., & Peletier, R. F., 1999, *MNRAS*, 310, 157
- Djorgovski, S., & Davis, M. 1987, *ApJ*, 313, 59
- Dressler, A., Lynden-Bell, D., Burstein, D., Davies, R. L., Faber, S. M., Terlevich, R. J., & Wegner, G. 1987, *ApJ*, 313, 42
- Durrell, P. R., Harris, W. E., & Pritchet, C. J. 1994, *AJ*, 108, 2114
- Durrell, P. R., Harris, W. E., & Pritchet, C. J. 2000, *AJ*, 121, 2557
- Elson, R. A. W. 1997, *MNRAS*, 286, 771
- Fall, S. M., & Efstathiou, G., 1980, *MNRAS*, 193, 189
- Forbes, D. A., Brodie, J. P., Grillmair, C. J., 1997, *AJ*, 113, 1652
- Freeman, K. C., 1970, *ApJ*, 160, 811
- Freeman, K. C. 1987, *ARA&A*, 25, 603
- Freeman, K. C. 1999, in *The Third Stromlo Symposium: The Galactic Halo*, eds. Gibson, B.K., Axelrod, T.S. & Putman, M.E., ASP Conference Series Vol. 165, p. 167
- Friel, E. D. 1995, *ARAA*, 33, 381
- Frogel, J. A., Tiede, G. P., & Kuchinski, L. E. 1999, *AJ*, 117, 2296
- Geisler, D., Lee, M. G., & Kim, E. 1996, 111, 1529
- Grillmair, C. J., Lauer, T. R., Worthey, G., Faber, S. M., Freeman, W. L., Madore, B. F., Ajhar, E. A., Baum, W. A., Holtzman, J. A., Lynds, C. R., O'Neil, E. J. Jr., & Stetson, P. B. 1996, *AJ*, 112, 1975
- Harris, G. L. H., Hesser, J. E., Harris, H. C., & Curry, P. J. 1984, *ApJ*, 287, 175
- Harris, G. L. H., Geisler, D., Harris, H. C., & Hesser, J. E. 1992, *AJ*, 104, 613
- Harris, W. E., 1991, *ARAA*, 29, 543
- Harris, W. E., 2001, in *Star clusters*, Saas-Fee Advanced Course 28. Lecture Notes 1998, Swiss Society for Astrophysics and Astronomy. Edited by L Labhardt and B. Binggeli. Published by Springer-Verlag, Berlin, 2001, p223.
- Harris, W. E., Harris, E. H., & Poole, G. B. 1999, *AJ*, 117, 855 (HHP)
- Harris, G. L. H., & Harris, W. E., 2000, *AJ*, 120, 2423 (HH00)
- Harris, W. E., & Harris, G. L. H., 2001, *AJ*, 122, 3065
- Harris, W. E., & Harris, G. L. H., 2002, *AJ*, 123, 3108 (HH02)
- Han, M.; Hoessel, J. G., Gallagher, J. S., III, Holtzman, J., Stetson, P. B. 1997, *AJ*, 113, 1001
- Holland, S., Fahlman, G. G., & Richer, H. B. 1996, 112, 1035
- Hui, X., Ford, H. C., Freeman, K. C., Dopita, M. A. 1995, *ApJ*, 449, 592
- Ibata, R., Irwin, M., Lewis, G., Ferguson, A. M. N., & Tanvir, N. 2001, *Nature*, 412, 49
- Kormendy, J., & Bender, R. 1996, *ApJL*, 464, 119
- Larsen, S. S., Brodie, J. P., Huchra, J. P., Forbes, D. A., Grillmair, C. J. 2001, *AJ*, 121, 2974
- Larson, R. B. 1975, *MNRAS*, 173, 671
- Lee, M. G., & Geisler, D. 1993, *AJ*, 106, 493
- Majewski, S. R. 1993, *ARA&A*, 31, 575
- Marleau, F. R., Graham, J. R., Liu, M. C., & Charlot, S. 2000, *AJ*, 120, 1779
- Martinez-Delgado, D., & Aparicio, A. 1998, *AJ*, 115, 1462
- McWilliam, A., & Rich, R. M. 1994, *ApJS*, 91, 749
- Minniti, D. 1996, *ApJ*, 459, 175
- Mould, J. 1984, *PASP*, 96, 773
- Mould, J., & Kristian, J. 1986, *ApJ*, 305, 591
- Peng, E. W., Ford, H. C., & Freeman, K. C. 2002, in preparation
- Perrett, K. M., Bridges, T. J., Hanes, D. A., Irwin, M. J., Brodie, J. P., Carter, D., Huchra, J. P., & Watson, F. G. 2002, *AJ*, 123, 2490
- Pritchett, C. J., & van den Bergh, S. 1999, *AJ*, 118, 883
- Reitzel, D. B., Guhathakurta, P., & Gould, A. 1998, *AJ*, 116, 707
- Reitzel, D. B., & Guhathakurta, P. 2000, *The Galactic Halo : From Globular Cluster to Field Stars*, Proceedings of the 35th Liege International Astrophysics Colloquium, held 5-8 July, 1999. Edited by A. Noels, P. Magain, D. Caro, E. Jehin, G. Parmentier, and A. A. Thoul. (Liege, Belgium : Institut d'Astrophysique et de Geophysique, 2000.), p.365
- Rejkuba, M., Minniti, D., Courbin, F., & Silva, D. R. 2002, *ApJ*, 564, 688
- Rich, R. M., Mighell, K. J., & Neill, J. D. Formation of the Galactic Halo...Inside and Out, ASP Conference Series, Vol. 92, 1996, Heather Morrison and Ata Sarajedini, eds., p. 544.
- Searle, L. & Zinn, R. 1978, *ApJ*, 225, 357
- Soria, R. et al. 1996, *ApJ*, 465, 79
- Sugimoto, D., Chikada, Y., Makino, J., Ito, T., Ebisuzaki, T., & Umemura, M. 1990, *Nature*, 345, 33
- Toomre, A., 1977, in *The evolution of galaxies and stellar Populations* ed. by B. Tinsley & R. Larson (New. Haven. CN: Yale

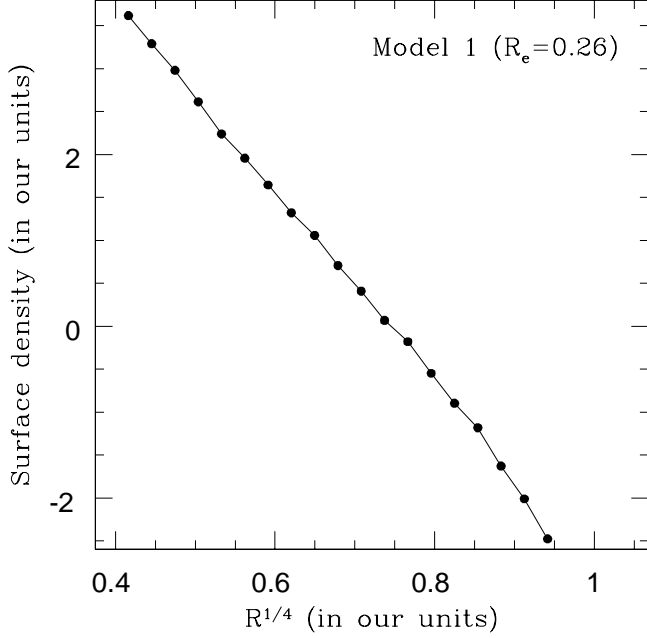


Figure 13. Surface density profile of the model M1. The profile of the simulated elliptical galaxy is well described as the $R^{1/4}$ law (de Vaucouleurs law) with the effective radius (R_e) of 0.26 ($R_e^{1/4} = 0.71$) in our units (corresponding to 4.6 kpc) in this model. This simulated profile is consistent with the observed one by van den Bergh (1976) for NGC 5128.

Vaucouleurs's law. The effective radius of the simulated elliptical galaxy in each model is 4.6 (M1), 4.6 (M2), 5.3 (M3), 6.1 (M7), and 7.0 kpc (M8). These derived values are not significantly different from the observed one. As is shown in Fig. 13, the simulated radial surface density profile in the model M1 follows de Vaucouleurs's law. The radial surface density profiles in other models can be also described as de Vaucouleurs's ones, which is consistent with the above observation (2). These comparison thus suggest that our model can reproduce the observed structural properties of NGC 5128 reasonably well.

- Univ. Press), p401
 van den Bergh, S. 1976, AJ, 208, 673
 van den Bergh, S. 1996, PASP, 108, 986
 van den Bergh, S., 1999, preprint (astro-ph/9908050)
 van den Bergh, S., 2000, in the galaxies in the Local group.
 Wielen, R., 1977, A&A, 60, 263
 Worthey, G., Trager, S. C., & Faber, S. M. 1996, ed. A. Buzzoni, A. Renzini, and A. Serrano, ASP Conf. Ser. Vol. 86, p. 203
 Wyse, R. F. G., Gilmore, G., & Franx, M. 1997, ARAA, 35, 637
 Zaritsky, D., Kennicutt, R. C., Huchra, J. P. 1994, ApJ, 420, 87

APPENDIX A: LIGHT PROFILES OF MERGER REMNANTS

Although the main purpose of this paper is not to discuss structural properties of NGC 5128, it is important for the present study to confirm whether our numerical simulations can reproduce not only the MDF observed in the NGC 5128 stellar halo but also its global structural properties. In the following, we assume that (1) the distance (d) of NGC 5128 is 3.9 Mpc (which is the same as that adopted in HH00 and HH02) and (2) the simulated density profile corresponds to the light profile (i.e., mass-to-light-ratio is constant for the entire region of a simulated elliptical galaxy). We then compare the observed radial brightness profile of NGC 5128 by van den Bergh (1976) with the simulated ones in models with initial dynamical conditions different with one another (i.e., M1, 2, 3, 7, and 8).

van den Bergh (1976) found that (1) the effective radius of NGC 5128 is about 5'.5 or ~ 6.2 kpc for $d = 3.9$ Mpc and (2) the radial brightness distribution follows de

Table A1. Model parameters

Model no.	M_b	metallicity gradient	$[m/H]_d$	orbit	f_h	$[m/H]_h$
M1	0.2	OC	-0.15	PR	0.05	-1.4
M2	0.6	OC	-0.15	PR	0.05	-1.4
M3	0.0	OC	-0.15	PR	0.05	-1.4
M4	0.2	GAS	-0.15	PR	0.05	-1.4
M5	0.2	OC	0.0	PR	0.05	-1.4
M6	0.0	OC	-0.15	PR	0.05	-1.4
M7	0.0	OC	-0.15	PP	0.05	-1.4
M8	0.0	OC	-0.15	RR	0.05	-1.4
M9	0.2	OC	-0.15	PR	0.20	-1.4
M10	0.2	OC	-0.15	PR	0.05	-2.0